

$S\ K\beta$ x-ray fluorescence spectra of the $Tl_2S - Sb_2S_3$ chalcogenide system

This article has been downloaded from IOPscience. Please scroll down to see the full text article.

1996 J. Phys.: Condens. Matter 8 8421

(<http://iopscience.iop.org/0953-8984/8/43/033>)

View [the table of contents for this issue](#), or go to the [journal homepage](#) for more

Download details:

IP Address: 171.66.16.207

The article was downloaded on 14/05/2010 at 04:25

Please note that [terms and conditions apply](#).

S K β x-ray fluorescence spectra of the Tl₂S–Sb₂S₃ chalcogenide system

S Dupont[†], A Gheorghiu[†], C Sénémaud[†], J-M Mariot[†], C F Hague[†],
P-E Lippens[‡], J Olivier-Fourcade[‡] and J-C Jumas[‡]

[†] Laboratoire de Chimie Physique–Matière et Rayonnement (Unité associée au CNRS),
Université Pierre et Marie Curie, 11 rue P et M Curie, 75231 Paris Cedex 05, France

[‡] Laboratoire de Physicochimie des Matériaux Solides (Unité associée au CNRS), Université
Montpellier II – Sciences et Techniques du Languedoc, Place Eugène Bataillon, 34095
Montpellier Cedex 02, France

Received 12 February 1996, in final form 1 July 1996

Abstract. The sulphur 3p valence states of Sb₂S₃, Tl₃SbS₃, TlSbS₂, TlSb₃S₅, TlSb₅S₈, and Tl₂S of the Tl₂S–Sb₂S₃ system have been investigated by means of the S K β (3p \rightarrow 1s) x-ray emission band. TlSb₃S₅ and TlSb₅S₈ were also studied in the glassy phase. Synchrotron-radiation-induced fluorescence was used. The spectra are discussed in terms of bonding between the sulphur atoms and their nearest neighbours with the help of tight-binding calculations. We observe significant differences among the S 3p states of all these materials, including between the crystalline and glassy phase of TlSb₃S₅. The variations in the S K β bandwidth and shape clearly reflect the sensitivity of the S 3p states to the local environment and indicate that the valence densities of states are mainly influenced by local order.

1. Introduction

Antimony chalcogenides have broad-ranging applications in optoelectronics [1] and as such represent an interesting class of compounds. The antimony atom, in its Sb³⁺ oxidation state, is characterized by the existence of a 5s² lone active electronic pair, which distorts its local environment and leads to complex and widely differing local structures. For example, in Sb₂S₃, Sb atoms exhibit two different sites with three and five S atoms as first neighbours [2]. The addition of a third more electropositive element such as Tl leads to changes in the environment of the Sb atoms and modifies the properties of the system. We have isolated four crystalline phases belonging to the Tl₂S–Sb₂S₃ system: Tl₃SbS₃ (25% Sb₂S₃ and 75% Tl₂S), TlSbS₂ (50% Sb₂S₃ and 50% Tl₂S), TlSb₃S₅ (75% Sb₂S₃ and 25% Tl₂S), and TlSb₅S₈ (83% Sb₂S₃ and 17% Tl₂S).

In this class of compounds, a wide range of optical and electrical properties are expected [3]. For instance, Tl₃SbS₃ is isostructural with Tl₃AsSe₃ [4,5] which is a semiconductor and exhibits nonlinear optical [6] and opto-acoustic [7] properties. It has a large transparency in the 1.23–18 μ m range and a high refractive index between 1.55 and 5.3 μ m.

Chalcogenide glasses are of special interest because of their ease of fabrication, with the possibility of being able to vary their composition to influence their properties [8]. In fact glassy Sb₂S₃ can only be obtained by means of a high cooling rate [9] and many studies have been concerned with solid solutions of Sb₂S₃ with other chalcogenides. Addition of

a modifier such as Tl_2S decreases the cooling rate required to form the glass. We have obtained glasses containing 5–35% Tl_2S by simply quenching the melt in water [10]. In this composition region, we synthesized two glass phases, g- TlSb_3S_5 and g- TlSb_5S_8 , with the same composition as the crystalline phases c- TlSb_3S_5 and c- TlSb_5S_8 .

Up to now, the atomic structure and the electronic properties of these compounds have been studied mainly by x-ray diffraction, Mössbauer spectroscopy, x-ray absorption spectroscopy and extended x-ray absorption fine-structure analysis [11–13]. Little experimental information exists concerning the valence densities of states (DOSs) [14, 15]. X-ray emission spectroscopy (XES) probes the occupied DOS with angular momentum and element selectivity. Our purpose was to search for modifications in the partial S 3p DOS as the structure varies in the Tl_2S – Sb_2S_3 system using the S $\text{K}\beta$ ($3\text{p} \rightarrow 1\text{s}$) emission from these ternary chalcogenides and the two binary compounds Tl_2S and Sb_2S_3 . The S $\text{K}\beta$ spectra of the two glasses were also recorded in order to obtain structural information by comparison with the crystalline phases. The XES data are discussed in relation to local environment and to tight-binding DOS calculations performed for TlSbS_2 and Tl_3SbS_3 .

2. Experiments

The binary chalcogenides Tl_2S and Sb_2S_3 were prepared by direct reaction of appropriate quantities of high-purity elements (99.999%). Ternary compounds were synthesized by mixing stoichiometric quantities of the binary compounds through solid state reaction at various temperatures according to the compound desired. TlSb_5S_8 was synthesized by recrystallizing amorphous TlSb_5S_8 [16]. The glasses were obtained by quenching the melt of the binary compounds in water following the procedure indicated in [13]. The materials were crushed into powders with about 5 μm granularity and stored in evacuated silica tubes.

The emission spectra were excited in the fluorescence mode with a polychromatic beam from a bending magnet beamline at the Super-ACO storage ring (LURE, Orsay). This excitation mode is specially suitable for reactive samples because it avoids contamination and chemical modifications of the samples during the measurements. The samples were prepared by depositing a thin uniform layer of chalcogenide powder onto adhesive tape. A specially designed bent crystal spectrometer [17] fitted with a 0.5 m radius ($10\bar{1}1$) quartz crystal ($2d = 0.66855$ nm) and a multichannel-plate 2D position-sensitive detector was used to record the data. Typical count rates were around 300 Hz over the whole spectrum. The energy resolution was about 1 eV.

3. The theoretical approach

We have used a tight-binding method based on the approach of Slater and Koster to calculate the DOS [18]. The choice was mainly dictated by the complexity of the crystal structures (for example up to 81 atoms in the Tl_2S unit cell). A previous tight-binding analysis of the ^{121}Sb Mössbauer isomer shift for antimony chalcogenides had shown the validity of this approach for these materials [19, 20]. Within the tight-binding approximation the S p-like DOS may be written

$$n_p(E) = \sum_k |\langle \varphi_p | \Psi_k \rangle|^2 \delta(E - E_k)$$

where φ_p is the 3p orbital of the sulphur atoms, E_k and Ψ_k are the energies and the wave functions at point k of the Brillouin zone. The summation is performed over the 3p orbitals of each of the sulphur atoms and 64 k -points of the Brillouin zone. We checked that

taking more k -points did not modify the results. As in [19,20], the present calculation was performed within the two-centre approximation. The one-centre parameters were taken as the energies of the neutral atoms calculated by Herman and Skillman [21]. For the two-centre parameters empirical forms according to Harrison [22] and Robertson [23] were considered and no significant differences were observed for the S p DOS. For simplicity we did not include interactions between thallium and sulphur in the calculation. This point will be discussed later.

The calculated p DOSs were convoluted with a Gaussian function of 2.5 eV full-width at half-maximum (FWHM) for easier comparison with the experimental data. This was the heuristic value used to broaden calculated molecular orbitals for comparison with very-high-resolution experiments on S₈ [24]. It is larger however than the combined effects of the core-level lifetime broadening, which is about 0.6 eV [25], and the experimental broadening, which is taken to be Gaussian in shape.

4. Results and discussion

S K β spectra of crystalline Tl₂S and Sb₂S₃ are compared in figure 1; those of crystalline Tl₃SbS₃, TlSbS₂, TlSb₃S₅, TlSb₅S₈, glassy TlSb₃S₅ and glassy TlSb₅S₈ are given in figure 2. All spectra are normalized with respect to the same maximum amplitude (peak A) and plotted on an x-ray transition energy scale. The overall shape of the S K β spectrum changes significantly from one compound to the other. In Tl₂S the S K β band (FWHM 3.6 eV) consists of a main band (A) and a well-resolved shoulder (C) located at about 4.1 eV to the low-transition-energy side of band A. The main S K β band in Sb₂S₃ appears to be much broader (FWHM 4.5 eV) due to the smaller energy separation between the peak (A) and the shoulder (B) and a larger B/A intensity ratio. The S K β spectrum of the ternary compounds also consists of the two well-resolved features. The spectrum for Tl₃SbS₃ is even narrower (FWHM 3.2 eV) than that of Tl₂S. The spectra of g-TlSb₃S₅, g-TlSb₅S₈ and c-TlSb₅S₈ are very similar but the crystalline phase of TlSb₃S₅ shows a narrower main peak as a result of a weaker lower transition energy structure. In table 1, we give the S K β peak and shoulder positions. The shoulder positions were estimated by systematically fitting two Voigt profiles only to the spectra (this is illustrated in figure 1). The procedure has no specific justification in relation to the S 3p partial DOS but it is useful for assessing the relative influence of bonding of the more tightly bound states in the various compounds.

Table 1. The energy position (eV) of the main peak (A) and its shoulder (B or C) given by the decomposition of the S K β spectrum.

Sample	A	B or C	A – (B or C)
Tl ₂ S	2465.8	2461.7	4.1
Tl ₃ SbS ₃	2465.8	2462.0	3.7
TlSbS ₂	2466.0	2463.2	2.8
c-TlSb ₃ S ₅	2466.1	2463.4	2.8
g-TlSb ₃ S ₅	2466.5	2464.1	2.4
c-TlSb ₅ S ₈	2466.4	2463.9	2.5
g-TlSb ₅ S ₈	2466.4	2464.0	2.4
Sb ₂ S ₃	2466.2	2463.7	2.6

The structural complexity of these compounds is of course closely related to the very large number of allotropes of sulphur [26] and the Sb 5s² lone pair. Sb₂S₃ is built from

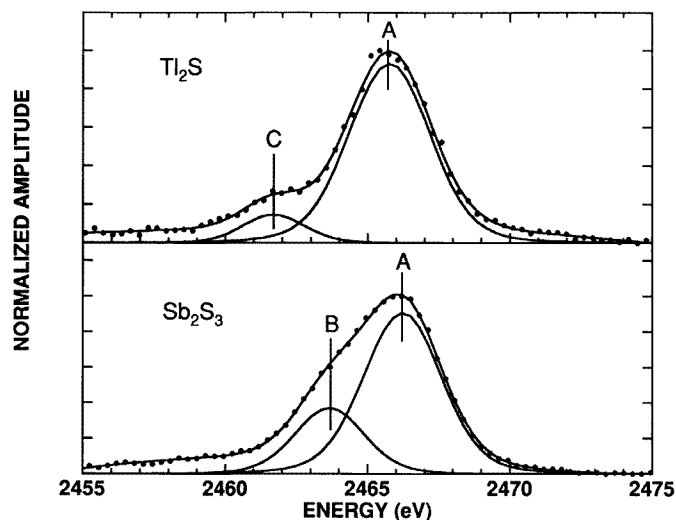


Figure 1. S $K\beta$ spectra of Tl_2S and Sb_2S_3 . The continuous line through the points is constructed from two Voigt profiles to indicate the shoulder position and a nonlinear background (not shown).

$(Sb_4S_6)_n$ double chains with Sb–S distances varying from 2.38 to 2.83 Å. As for Tl_2S , it has a layered structure, similar to that of CdI_2 . In CdI_2 , the layers are connected by anion–anion bonds, whereas the layers are connected by cation–cation bonding in Tl_2S . The thallium atoms lie at six different pyramidal sites. Each sulphur atom is surrounded by six Tl atoms but lies at five distinct crystallographic sites. The Tl–S distances vary from 2.5 to 3.3 Å [27]. Details of the crystallographic structure of the ternary materials have been published elsewhere [4, 28–30]. Tl_3SbS_3 has the simplest structure with just one crystallographic site for each element. The Tl–S bond length is 3.03 Å. Sulphur has only one antimony nearest neighbour at 2.43 Å, but each Sb atom has three nearest neighbour sulphur atoms [4]. $TlSbS_2$ also has relatively short Sb–S distances (2.5 Å). This time Sb has two and S has four different sites. The Tl–S distance of 3.1 Å is similar to that of Tl_3SbS_3 . In $TlSb_3S_5$, sulphur has five different crystallographic sites. Each S has two Sb nearest neighbours on average at an average Sb–S distance of 2.54 Å. Each S atom has one Tl nearest neighbour at an average distance of 3.17 Å [28]. Finally there are 16 different crystallographic sites for sulphur in $TlSb_5S_8$ with large Tl–S bond lengths (3.25 Å) for an average of 0.75 nearest neighbour. The 2.2 Sb nearest neighbours, on average, have covalent Sb–S bonds (2.56 Å). It is interesting to note that the sum of the Sb–S covalent radii is 2.4 Å whereas the sum of the Tl–S ionic radii is 3.3 Å. Information concerning the local environment of sulphur atoms is given in table 2.

Moving down the group IIIB elements from aluminium to thallium, the overlap between the s and p valence states diminishes to the point at which a gap opens between the s and p bands in Tl. Note that the s-like states are centred around 6 eV so that the overall valence band width is similar to that of aluminium. The Tl 6p states form a narrower peak close to the Fermi energy (E_F). Going across the periodic table from the group IIIB to group VIB elements, the overlap between s and p states also decreases. This time it is a consequence of the increased binding energy of the s-like states. The most studied allotrope of sulphur is S_8 . X-ray photoelectron spectroscopy (XPS) experiments [31] indicate that the S 3s states contribute to the bonding but are tightly bound (10–20 eV binding energy). This has also

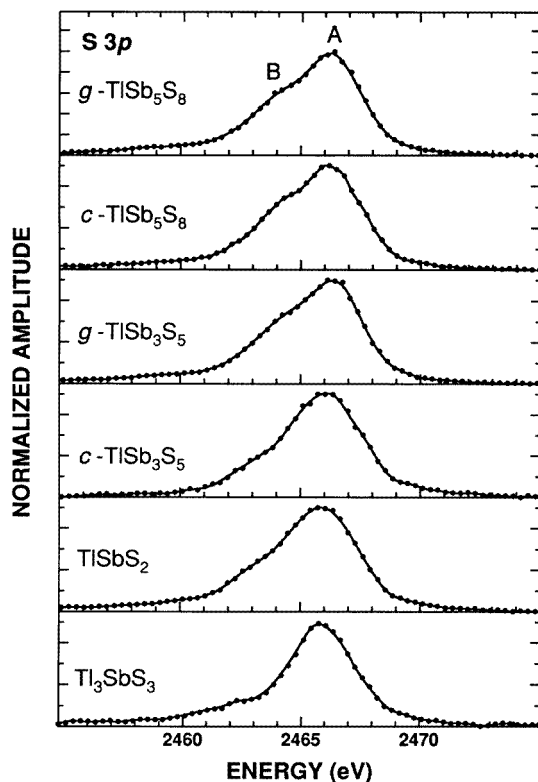


Figure 2. S K β spectra of crystallized and glassy compounds of the Tl₂S–Sb₂S₃ system.

Table 2. Local environments of sulphur atoms.

Sample	Number of S sites	Average number of first Sb neighbours	Average Sb–S bond length (Å)	Average number of first Tl neighbours	Average Tl–S bond length (Å)
Tl ₂ S	5			3.0	2.87
Tl ₃ SbS ₃	1	1.00	2.43	3.0	3.03
TlSbS ₂	4	1.75	2.55	2.5	3.17
TlSb ₃ S ₅	5	2.0	2.54	1.0	3.17
TlSb ₅ S ₈	16	2.2	2.56	0.75	3.25
Sb ₂ S ₃	3	2.7	2.64		

been confirmed by S K β and L_{2,3} XES spectra [24]. Antimony occupies an intermediate position between sulphur and thallium with a relatively narrow 5p band and with 5s states centred at about 7 eV binding energy.

With some Tl–S distances as short as 2.5 Å in Tl₂S, this compound should show some overlap between the respective p orbitals. In fact what is unambiguously observed is hybridization between S 3p and Tl 6s states (peak C). Tl₂S XPS measurements [32] confirm that the S p-like band has a FWHM of about 3.5 eV and an s-like band situated about 4.5 eV below the p-peak, namely 6 eV below E_F . The origin of shoulder B in Sb₂S₃, on the other hand, must be the result of hybridization between S 3p and Sb 5p states, whereas the main peak belongs mainly to non-bonding S 3p states.

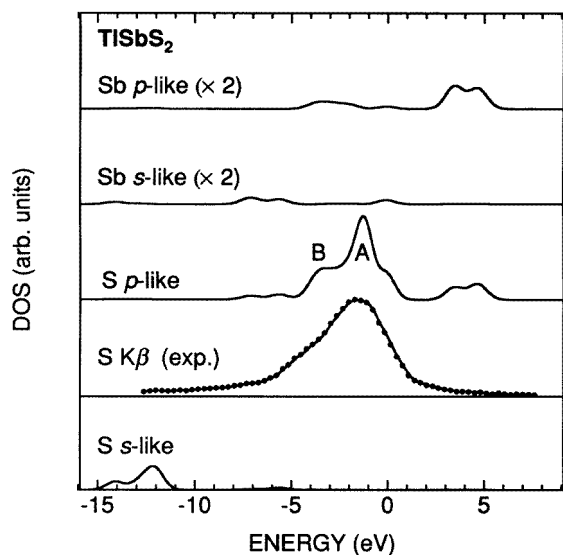


Figure 3. The S K β spectrum of TlSbS₂ and partial densities of states for S and Sb.

The analogy between these binary compounds and the ternary compounds is clear. Starting with Tl₃SbS₃ which has the highest thallium content, we observe a well-defined shoulder at C which we attribute to the S 3p–Tl 6s hybridization. Peak A is narrower than that in Tl₂S which could mean that covalent bonding between Tl 6p and S 3p states is weaker due to the absence of short Tl–S bond lengths. The single Sb atom has little impact on the shape of the spectrum.

Compared to Tl₃SbS₃, the thallium content in TlSbS₂ is roughly halved but the Sb content increased. Each S has 2.5 nearest-neighbour Tl sites. This gives rise to a fairly intense shoulder B situated closer to peak A. The Tl 6s–S 3p hybridization has obviously weakened while the Sb–S covalent bonding contributes to the structure. The width of peak A is little changed despite the four distinct sulphur sites. This is not unexpected because the x-ray emission from each type of site measures the difference in energy between the S 1s core hole and the valence states. A change in core-level binding energy involves a compensating change in screening by valence electrons at each type of site, thus cancelling out broadening effects. The same can be said for TlSb₃S₅ with its five different sulphur sites. Shoulder B in TlSb₃S₅, however, is weaker than expected compared to the glassy phase and to TlSbS₂ with its lower Sb content. c-TlSb₅S₈ again shows a strong shoulder at B. In this case the glassy and crystalline compounds are indistinguishable. As pointed out above, even the crystalline compound has 16 different crystallographic sites so it is hardly surprising that the glassy state does not have a different spectrum. Coming back to TlSb₃S₅, it is interesting to note that this compound can be described roughly as consisting mainly of (SbS₄)_n ribbons. ¹²¹Sb Mössbauer measurements [33] indicated that the glass is made up of fragments of ribbon. The effect of disorder or more generally increasing the number of different crystallographic sites according to our XES measurements is to increase the covalent bonding between the Sb and S p-like states.

The model calculations performed for TlSbS₂ (figure 3) and Tl₃SbS₃ (figure 4) tend to confirm our qualitative interpretations since they indicate that the Sb–S interaction is dominated by p-bonding. Sb s-like states are not predicted to hybridize with the S p-like

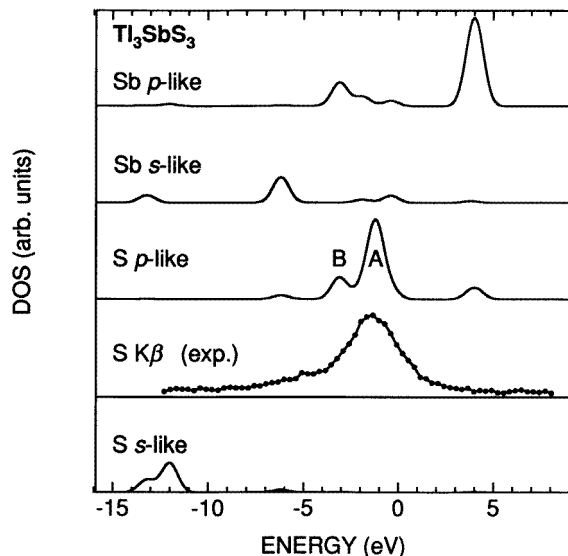


Figure 4. The S K β spectrum of Tl₃SbS₃ and partial densities of states for S and Sb.

states. The main peak in the calculated DOS corresponds to non-bonding S states. Lone electron pairs are expected in chalcogenides with twofold coordination. They have indeed been observed in XPS spectra of S₈ thin films [31] as a weakly bound peak about 2 eV below E_F . The S p-like bonding states lie about 5 eV below E_F . The complex bonding of these compounds certainly explains that no clearly identifiable structure attributable to lone pairs is observed in these S K β spectra. The main difference between the S p-like states in Tl₃SbS₃ and those in TlSbS₂ according to the tight-binding calculation is the absence of a shoulder to the low-binding-energy side of A. This was not confirmed by the shape of the S K β spectrum but, as mentioned in section 3, the calculation neglected Tl 6p states. These very probably contribute to the signal at low binding energies, further masking any lone-pair-related structure. The structure to the low-energy side of peak A in TlSbS₂ (figure 3) is echoed by small features in the Sb s-like and p-like states according to the calculation. Though not resolved experimentally, its presence may explain that the DOS are not steeply sloped towards E_F .

The optical gap in the Tl-rich compounds is in the range 1.2–1.3 eV but in the other compounds it increases to about 1.5 eV. This is no doubt as a result of the increased Sb-S covalency observed here.

5. Conclusions

The S K β emission band of crystalline and glassy materials of the Sb₂S₃–Tl₂S system measured in the fluorescence mode using synchrotron radiation reveals significant changes in the S 3p electronic structure as relative Tl and Sb contents are modified. A tight-binding calculation shows that the main features of the spectra of the antimony compounds can be assigned to non-bonding S 3p states. Bonding states, essentially consisting of hybridized S and Sb p-like states, are very sensitive to local environment and to disorder. In the case of TlSb₅S₈, which has the most complex structure with 16 different sulphur sites, there is

no difference between the ordered and disordered phases. However, TlSb_3S_5 with only five different sulphur sites does show a significant change in its electronic structure. This means that quenching a particular composition may lead to modified physical properties relative to the equivalent crystalline phase.

Acknowledgments

We would like to thank the staff of Super-ACO. The experiments were performed on beamline SB3 belonging to the Commissariat à l'Energie Atomique, Département des Mesures, Centre d'Etudes de Bruyères-le-Châtel.

References

- [1] Goodman C H L 1985 *Mater. Res. Bull.* **20** 237
- [2] McKee D O and McMullan J T 1975 *Z. Kristallogr.* **142** 447
- [3] Ibañez A, Fourcade J, Jumas J C, Philippot R and Maurin M 1986 *Z. Anorg. Chem.* **540/541** 106
- [4] Rey N, Jumas J C, Olivier-Fourcade J and Philippot E 1984 *Acta Crystallogr. C* **40** 1655
- [5] Hong H Y-P and Mikkelsen Jr J C 1974 *Mater. Res. Bull.* **9** 365
- [6] Feichtner J D and Roland G W 1972 *Appl. Opt.* **11** 993
- [7] Gottlieb M, Isaacs T J, Feichtner J D and Roland G W 1974 *J. Appl. Phys.* **45** 5145
- [8] Dubois B, Portier J and Videau J-J 1984 *J. Optique* **15** 351
- [9] Červinka L and A Hrubý A 1982 *J. Non-Cryst. Solids* **48** 231
- [10] Durand J M 1994 *Thesis* Montpellier
- [11] Olivier-Fourcade J, Ibañez A and Jumas J C 1990 *J. Solid State Chem.* **87** 336
- [12] Olivier-Fourcade J, Ibañez A, Jumas J C, Dexpert H, Blancard C, Esteva J-M and Karnatak R C 1991 *Eur. J. Solid State Inorg. Chem.* **28** 409
- [13] Durand J M, Lippens P E, Olivier-Fourcade J, Jumas J C and Womes M 1996 *J. Non-Cryst. Solids* **194** 109
- [14] Lampre I, Gheorghiu A, Sénémaud C, Lippens P E, Durand J M, Olivier-Fourcade J, Lefebvre I and Lannoo M 1993 *Proc. 16th Int. Conf. on X-Ray and Inner-Shell Processes (Debrecen, 1993)* ed L Sarkadi and D Berenyi
- [15] Gheorghiu A, Lampre I, Dupont S, Sénémaud C, El Idrissi Raghni M A, Lippens P E and Olivier-Fourcade J *J. Alloys Compounds* 1995 **228** 143
- [16] Jumas J C, Olivier-Fourcade J, Rey N and Philippot E 1985 *Rev. Chim. Minérale* **22** 651
- [17] Hague C F and Avila A 1996 to be published
- [18] Slater J C and Koster G F 1955 *Phys. Rev.* **94** 1498
- [19] Lefebvre I, Lannoo M, Allan G, Ibañez A, Fourcade J, Jumas J C and Beaufort E 1987 *Phys. Rev. Lett.* **59** 2471.
- [20] Lefebvre I, Lannoo M, Allan G and Martinage L 1988 *Phys. Rev. B* **38** 8593
- [21] Herman F and Skillman S 1963 *Atomic Structure Calculations* (Englewood Cliffs, NJ: Prentice-Hall)
- [22] Harrison W A 1980 *Electronic Structure and Properties of Solids* (San Francisco: Freeman)
- [23] Robertson J 1983 *Phys. Rev. B* **28** 4671
- [24] Kortela E-K, Suoninen E, Karras M and Mannes R 1972 *J. Phys. B: At. Mol. Opt. Phys.* **5** 2032
- [25] Krause M O and Oliver J H 1979 *J. Phys. Chem. Ref. Data* **8** 329
- [26] Meyer B 1976 *Chem. Revs.* **76** 367
- [27] Man L I *Sov. Phys. Crystallogr.* **15** 399
- [28] Gostojic M, Nowacki N and Engel P 1982 *Z. Kristallogr.* **159** 217
- [29] Rey N, Jumas J C, Olivier-Fourcade J and Philippot E 1983 *Acta Crystallogr. C* **39** 971
- [30] Engel P 1980 *Z. Kristallogr.* **151** 203
- [31] Salaneck W R, Lipari N O, Paton A, Zallen R and Liang K S 1975 *Phys. Rev. B* **12** 1493
- [32] Porte L and Tranquard A 1980 *J. Solid State Chem.* **35** 59
- [33] Olivier-Fourcade J, Jumas J C, Rey N, Philippot E and Maurin M 1985 *J. Solid State Chem.* **59** 174